URBAN GROWTH STUDIES FOR JOHANNESBURG CITY USING REMOTELY SENSED DATA

Priyanka Verma, Piyush Yadav, Shailesh Deshpande, Jayavardhana Gubbi, Balamurali P
Tata Research Development and Design Center (TRDDC),
TCS Innovation Labs, Pune, India
Email: {priyanka.32, piyush.yadav1, shailesh.deshpande, j.gubbi, balamurali.p}@tcs.com

KEYWORD: SVM, VIS Classification, LULC, Urban Growth, Remote Sensing

ABSTRACT: Johannesburg is the largest city of Gauteng province of South Africa characterized by dual urban structure, which leads to growth in urbanization. Employment opportunities have led to migration of skilled and unskilled workers from national frontiers and provincial borders of Gauteng. Land Use Land Cover (LULC) change analysis have been one of the conventional methods for analysing the impact of anthropogenic activities. This paper analyses patterns of LULC, anticipate the impervious surface growth and green cover loss in the Johannesburg city. Changes in various LULC classes namely residential, industrial, forest, shrubs, water bodies, burnt soil, open areas etc. were evaluated using Landsat imagery from 2000 to 2016. Remotely sensed images were classified in to different classes by Support Vector Machine (SVM). Further, these classes have been grouped into broad level classes such as impervious surface (I), vegetation (V), and soil (S). Based on VIS classification, land change analysis was done where results shows that impervious surface has increased by 57.03% from 2000 to 2016, which resulted in loss of urban vegetation (grass, tress cover etc.), and agricultural land by 47.8%, soil and water loss was 16.75%.

1. INTRODUCTION

Southern African cities are characterized by dual urban structure. This structure was inherited from the colonial systems where semi-urbanized areas coexist with the urban areas, comprised of proper living conditions. Semi-urbanized areas have insufficient basic facilities and infrastructure, where majority of population having the low income. According to a recent survey released in Johannesburg by South African Institute of Race Relations (SAIRR), only 33% of total population now lives in rural areas (SOUTH-AFRICA, 2016). The number of people living in rural areas was decreased from 48% to 38% in the span of 11 years, whereas urban area population increased from 52% to 62%. SAIRR identified the major precipitate of the trend as higher economic growth in urban areas and the post-apartheid freer movement of people which attracted people, searching for employment.

Johannesburg is the wealthiest as well as the largest city of Gauteng province of South Africa. It stands in top 50 urban areas of the world. Being the economic powerhouse of the continent along with the dual urban structure, it is destination of choice for workers from all over the continent. All these factors contribute towards rapid urbanization of the city. The unanticipated increase in the urbanization, inadequate planning, and development has created an extensive pressure on cities resources both natural and economic (Schaffler & Swilling, 2013). Various buildings

and townships have been raised over agriculture lands increasing the buildup areas. Along with main city, urban sprawl is also increasing in the outskirts. Hence, it is necessary to understand the complex interaction between rapidly growing urban agglomerate of Johannesburg, South Africa and its surrounding biophysical systems.

In this paper we present the urban growth analysis of Johannesburg, South Africa. We performed LULC classification of remotely sensed data and then detected changes in VIS classes for the city over a ~decade. The temporal intra-class transitions of VIS classes for Johannesburg was considered to model the urban growth. Further paper is divided into four sections: "Materials and Methods" section elaborates study area, methods used for data collection and its preprocessing along with classification methodology, "Experimental Results" provides analysis of classification results and statistics about growth, "Conclusion" summarizes the interesting observation of the study.

2. MATERIALS AND METHODS

Various steps involved in urban growth prediction are summarized in Figure 1. Data selection involves choice of area and collection of respective data required for the analysis. It is further processed in data pre-processing step to achieve better results at the end. Finalised data is classified using supervised classification algorithm and given as input for LULC prediction which is performed by TERRSET module using various driver variables.

2.1 Study Area

Johannesburg is located at an elevation of 1,753 meters (5,751 ft.) in eastern plateau area of South Africa known as the Highveld which has a subtropical highland climate. The eastern part of the city are flatter while north and west part have hills all over. It is the hub of South Africa's financial, commercial, mining, and industrial undertakings. The land area of the city is large when compared to other major cities of South Africa, 1,645 km2 (635 sq. mi), resulting in population density of 2,364/km^2. The study area consists of many Johannesburg Central Business Districts (CBD). Selected area represents all the important physical features and landmark of the city, with top leftmost corner as (Lat: -26.5257765, Long: 27.7131012) and bottom rightmost corner as (Lat: -25.9032623, Long: 28.2248505) (Figure 2).

2.2 Data Collection And Preprocessing

Landsat 7 images were used in this study. The images taken for analysis were considered from USGS Earth Explorer (USGS, 2015). Longer duration is required to study urban growth pattern, hence we looked at time frame of year 2000 to 2016. Year 2012 was not considered due to unavailability of clear imagery.

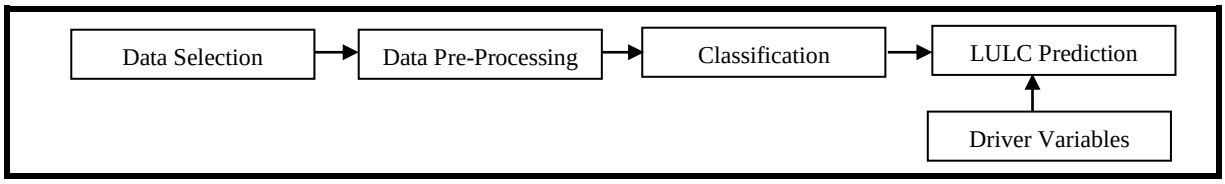

Figure 1 Steps for Urban Growth Prediction

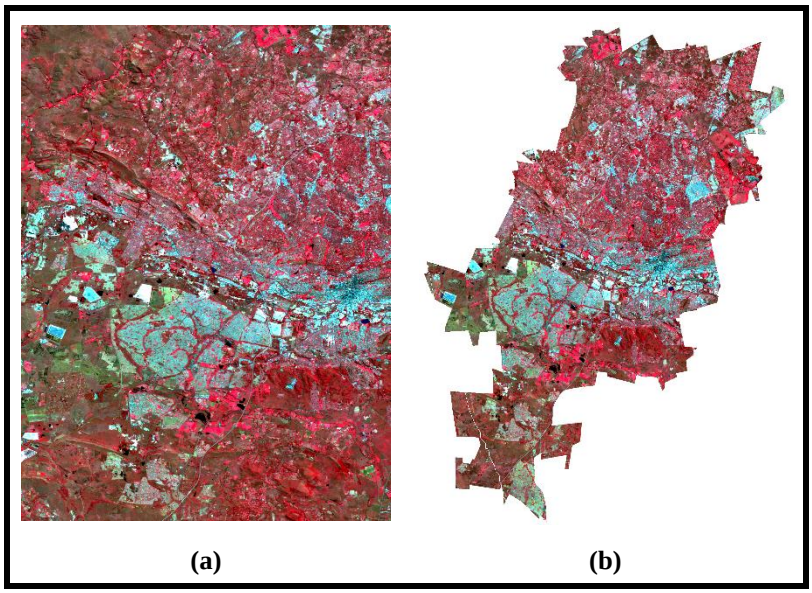

Figure 2 (a) Study Area (USGS, 2016), (b) Johannesburg Administrative Boundary

Gathered data for remaining years was preprocessed and corrected to make it suitable for analysis (Figure 3).

2.2.1 LANDSAT 7 Images

Landsat 7- ETM+ acquired images have spatial resolution of 30 (Band 1-7) and 15 m (Band 8) respectively. All bands can collect high or low gain settings for increased radiometric sensitivity and dynamic range, where Band 6 can collect both gain settings for all scenes. Approximate scene size is 106 mi by 114 mi. Images considered for analysis have been taken by LANDSAT 7 satellite with Enhanced Thematic Mapper Plus (ETM+) sensors (USGS, 2016) in the month of March and April. Particularly these months were selected as clear sky is observed in this time period which provides the clear visibility of city in images. Different preprocessing techniques were applied for correcting of images (Figure 3).

2.2.2 Scan Line Correction (SLC)

In some images, scan lines were observed due to failure of Scan Line Corrector (SLC) of ETM sensor in 2003 (LANDSAT-7, 2016). Sliding window approach was used to remove these black scan lines as shown in Figure 4.

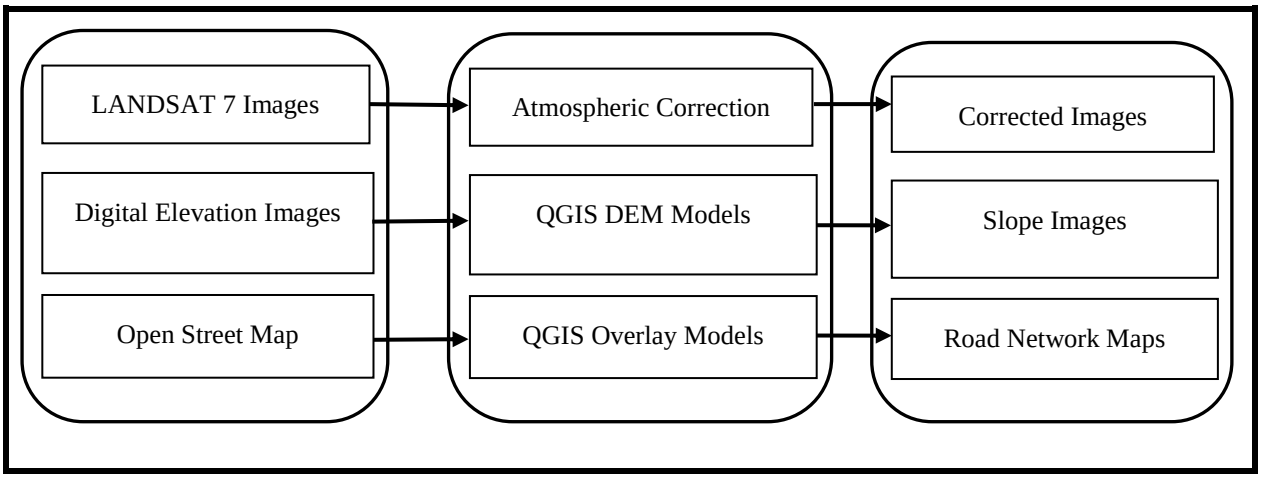

Figure 3 Data Processing Steps for Correcting Images

Let us consider an image *I* of size *4X5* with pixels labeled defined classes. The scan line pixels were given the label 5. Sliding window of size *3X3* was traversed over the image *I*. If center of window overlapped with SLC pixel, count of each unique class was calculated in that particular window. The class label with the highest count will replace the center value. The size of window depends on the width of SLC lines. Thicker the lines larger will be the window size.

2.2.3 Atmospheric Correction

Electromagnetic radiations is attenuated by atmospheric inference, caused due to absorption and scattering. Path radiance method was used for the atmospheric correction of LANDSAT data. The digital number (DN) of water pixel in band 4 (infrared band) was subtracted from all DN values of images. Infrared band was selected due to its near to 0 water leaving radiance. New obtained DN values were then converted to spectral radiance using Eq. 1 (Kaufman, 1989)

$$L = L_{min} + \left(\frac{L_{max}}{254} - \frac{L_{min}}{255}\right) x\, DN \tag{1}$$

Where, L , L_{min} and L_{max} represents radiance, minimum and maximum radiance values respectively. DN shows the recorded digital number at the sensor.

Radiance to reflectance conversion of the DNs was performed to normalize the other atmospheric effects such as solar elevation, irradiance etc. Normalization was done by using Eq. 2 (Kaufman, 1989), where the spectral radiance was converted to exoatmospheric reflectance.

$$\rho_p = \frac{\pi \,.\, L_\lambda . d^2}{ESUN_\lambda . \cos\theta_s} \tag{2}$$

Where, ρ_p= planetary reflectance, L_λ = radiance, d = distance between earth and sun, $ESUN_\lambda$ was mean solar

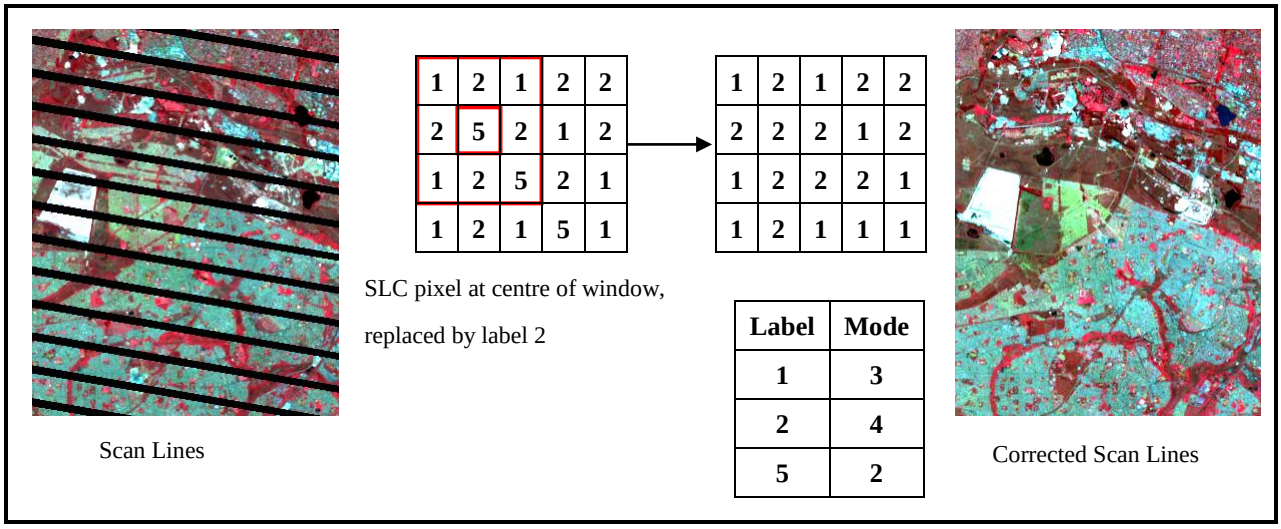

Figure 4 Sliding Window Approach for correcting scan lines (Yadav, Deshpande, 2015)

exoatmospheric irradiance, and θ_s as solar zenith angle.

2.2.4 Digital Elevation Image (DEM)

The elevation or slope of the surface is important parameter that determines potential of urban growth. DEM images were acquired from the CARTOSAT-1 satellite, launched and maintained by Indian Space Research Organization (ISRO). This satellite carries two panchromatic (PAN) cameras with spatial resolution of 2.5 m (BHUVAN, 2016). The DEM image has been converted to slope using QGIS DEM Terrain models (GDAL_PROXIMITY, 2016) (Figure 5), which has used in HMM for urban growth prediction.

2.2.5 Road Network Image

Road networks and growth share a complex relation with each other. Highly developed area can lead to efficient road networks, and good road networks can also contribute towards the development. In this work, road network image was used for future growth prediction. The road network for the present work was acquired from Open Street Maps (OPENSTREETMAP, 2016). Only Primary-motorway roads were considered for assessment due to their significant impact on the economy (Figure 5 (c)). Obtained network was converted to raster distances with the use of QGIS proximity raster distance (GDALDEM, 2016) and used as input in urban growth prediction model.

2.3 Classification Methodology

Pre-processed LANDSAT images were classified into fourteen different classes (Figure 5). SVM (Cortes, Corinna, & Vapnik, 1995) algorithm was used to classify each pixel of image in to various thematic classes. To achieve the highest accuracy of classification texture measure of image was also taken into consideration. Local Binary Pattern algorithm (LBP) was used to detect the texture by measuring LBPs over an image (Scikit-LBP, 2016).

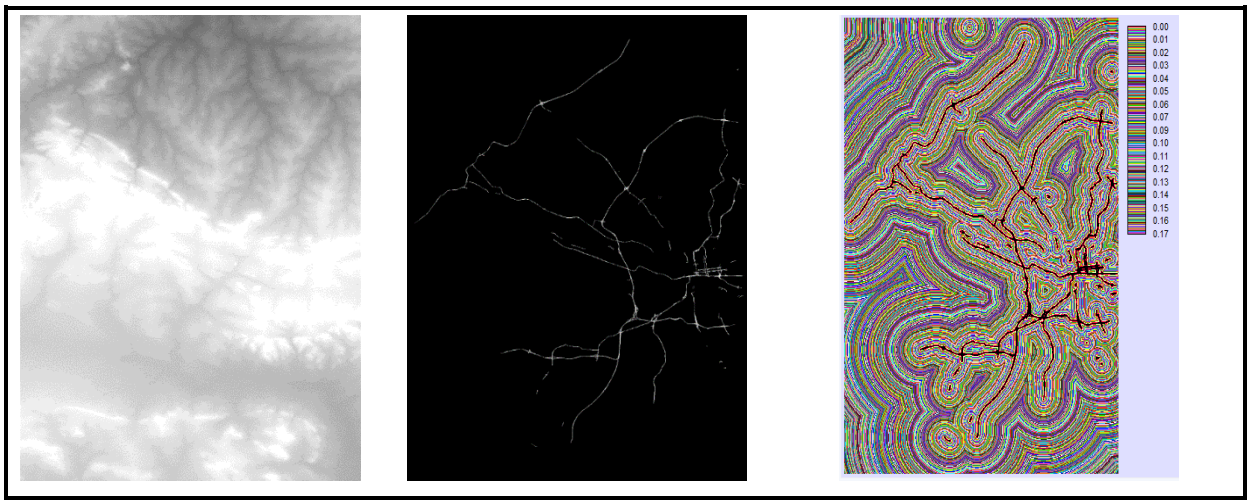

(a) (b) (c)

Figure 5 a) DEM data b) Primary-Motorway c) Road Distance Matrix

Training and testing datasets were created manually for each class. It was done by extracting corresponding pixel values from the image. SVM algorithm provide better results in classification of remote sensed data, when compared with Naïve bayes and nearest neighbour algorithm (Yadav & Deshpande, 2015). Hence, in our analysis, SVM classifier was used for classification. Figure 5 shows classification results. Impervious surface and bright soil were having little resemblance in signatures, thus lead to some miss classification. This type of misclassification was corrected manually (5%) with help of google maps (Google-Maps, 2016). Finally, 11 classes were grouped into four classes Vegetation, Impervious, Soil, and Water (VIS) Figure 7(c).

The land use change modelling approach (Markov-CA approach) implemented by TERRSET module (TERRSAT-LCM, 2016) provides ways for estimating different future scenarios. Markov-CA modelling approach was used to predict land use in 2016 and 2020 by extrapolating current trends. The classified images have been taken as the input along with the road data, slope data and various other driver variables for CA modelling. Driver variables include Gross Domestic Product, Interest Rate Cycle, Total Road Length Added, Per capita Electricity Consumption, and Consumer Price Index Inflation (WORLD-BANK, 2016). These variables were used to calculate the transition probabilities for 2016 and 2020 in TERRSET module.

3. EXPERIMENTAL RESULTS AND DISCUSSION

VIS analysis of the city revealed rapid urbanization in Johannesburg city for past 16 years (2000-2016). The fringes of the city were developed much more rapidly than the core city due to land availability for the public and private infrastructure. Table 1 represents VIS changes happened in the last 16 years. Consistent increase in impervious surface was observed (Table 1) and vegetation pixels shows continuous decreasing trend. In 2000 the impervious surface was 16.08% of total study area whereas it rose to 22.14% in 2004, to 23.81% in 2008 and in 2016 build area reached to 26.41%. Thus, there was total increase in built up area by 10.33% of total area and 57.04 % of

impervious surface in 2000 to 2016. As expected, in last 16 years, vegetation was decreased by 47.80% of agriculture land existing in 2000 in last sixteen years. Rates of decrease in vegetation was likely to be associated with developments in technology and growth of human population. Variation in soil and water was also observed due to seasonal land cover changes.

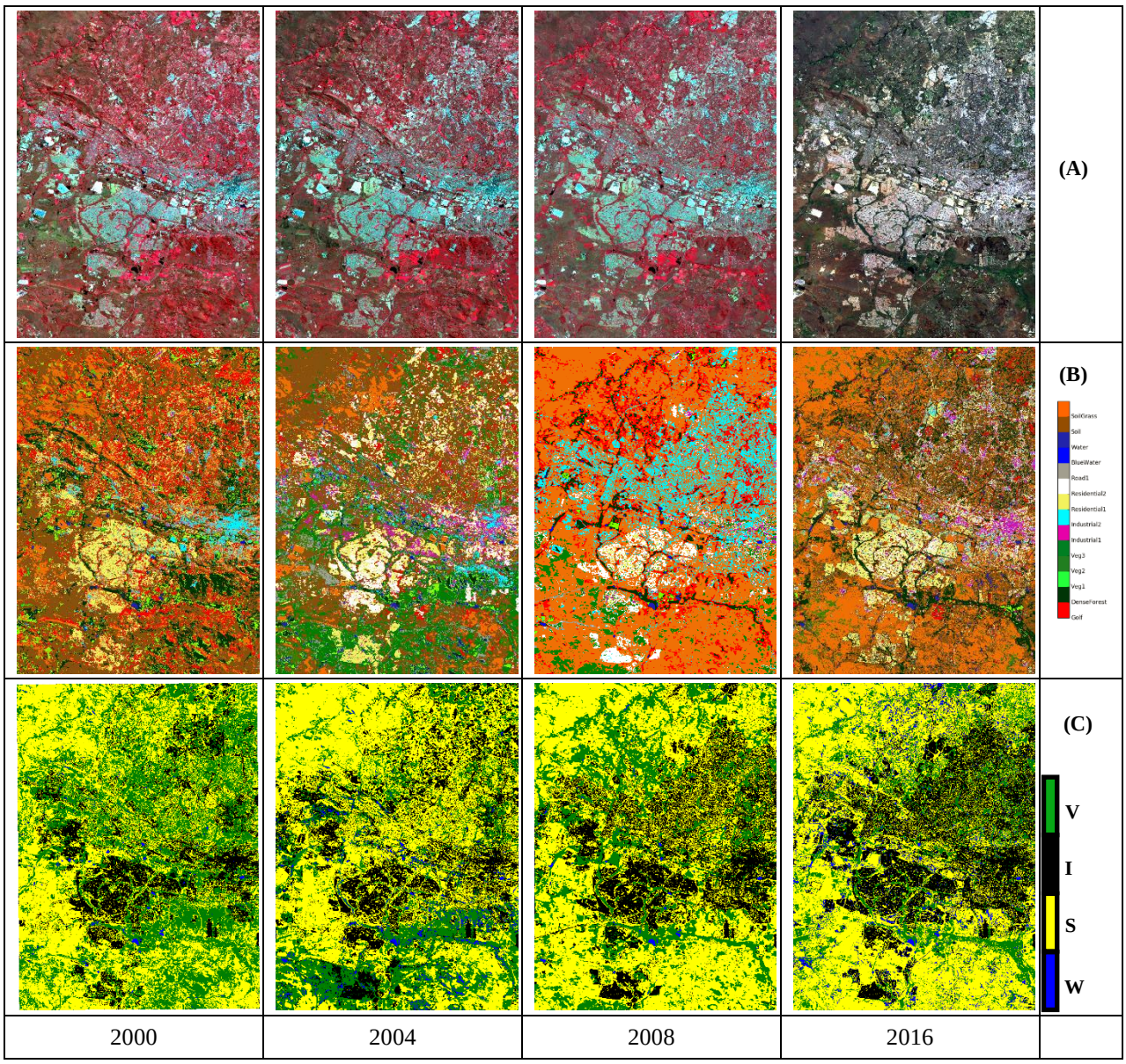

Figure 6 Johannesburg LULC Classification, A) Satellite Image (USGS, 2016), B) Classified Images and C) VIS Classified Image

Table 1 Year Wise Number of Pixels Corresponding to VIS Classes

	2000	**2004**	**2008**	**2016**
Vegetation	856852	589079	557054	447283
Impervious	395396	520696	559821	620919
Soil	1087247	1197479	1226626	1180299
Water	11582	43823	7576	102576

TERRSET module was successful in predicting built up area in 2016 and the results were comparable to actual LULC for 2016. Figure 8 represents prediction of 2020 impervious surface along with conversion chances of one class to another. In projected transaction potential black colour represents resistant to change and as we go from orange to red colour, class has high probability of conversion to impervious surface. The projected LULC for 2020 unveil more urbanization of the landscape with growth in residential areas.

4. CONCLUSION

This paper aims at analysing LULC changes occurred in Johannesburg, South Africa between 2000 and 2016 using remotely sensed data and GIS. Further, the paper provides detailed account of LULC dynamics of the city along with LULC prediction for year 2020. The main change observed was prominent increase in impervious surfaces, from 16.08% to 26.41% of total study area which is mainly result of the migration of population from rural to urban areas (Schaffler & Swilling, 2013). Increase in built up area has resulted in loss of agricultural land from 36.44% to 19.02% with a total loss of 17.42%. LULC prediction and validation was done for 2016 and outcome was found to be comparable with the ground truth (~80%). The results and methodology is not only useful for urban growth studies and changes detection but also for natural resource management as well.

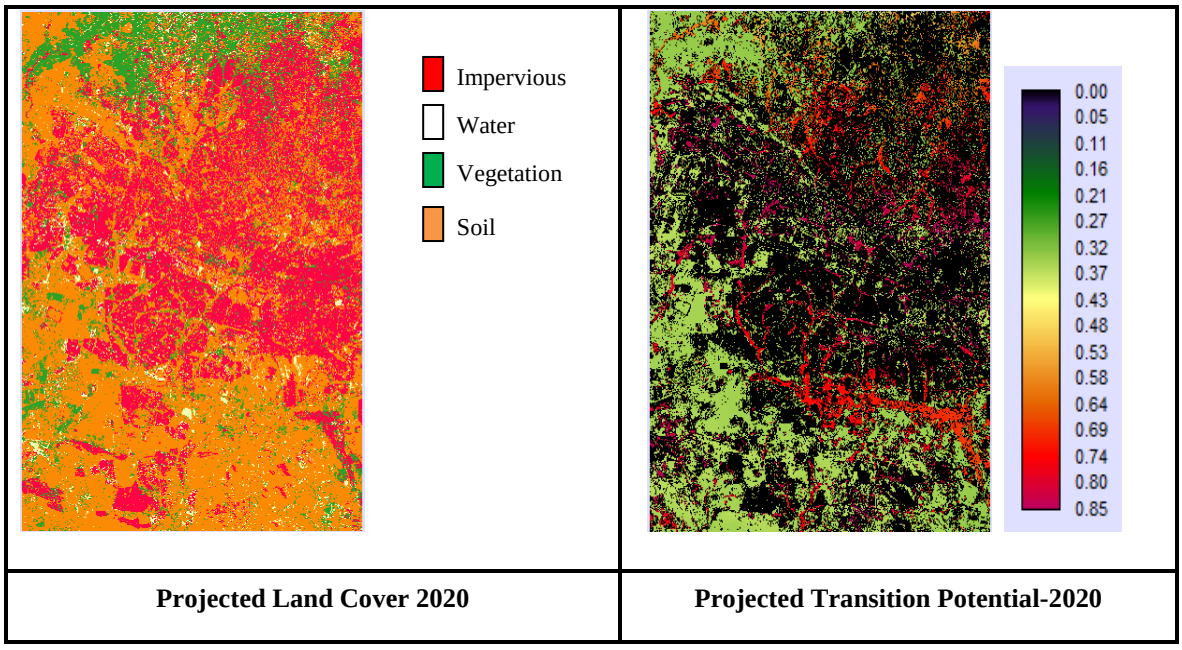

Figure 7 : LULC Prediction of Year 2020

Table 2: Transition Matrix of VISW for Year 2020

	I	W	V	S
I	0.85	0.018	0.05	0.081
W	0.002	0.775	0.093	0.129
V	0.106	0.024	0.047	0.396
S	0.08	0.018	0.115	0.787

5. REFERENCES

BHUVAN. (2016). Bhuvan: Gateway of Indian Earth Observation. Retrieved May 1, 2016, from http://bhuvan.nrsc.gov.in/data/download/index.php

Cortes, Corinna, Vapnik, V. (2016). Support-vector networks. Machine Learning. Springer, 20(3), pp. 273-297.

Cracknell, A. (2007). Atmospheric Corrections to Passive Satellite Remote Sensing Data. In: Introduction to Remote Sensing, pp. 196.

GDAL_PROXIMITY. (2016). Retrieved May 1, 2016, from http://www.gdal.org/gdal_proximity.html

GDALDEM. (2016). GDALDEM. Retrieved May 4, 2016, from www.gdal.org/gdaldem.html

Google_Earth. (2016). Google Earth. Retrieved May 1, 2016, from https://www.google.com/earth/

HARRIGEOSPATIAL. (2016). HARRIGEOSPATIAL. Retrieved May 4, 2016, from http://www.harrisgeospatial.com/docs/AtmosphericCorrection.html.

Kaufman, J. Y. (1989). The atmospheric effect on remote sensing and its correction. In: Theory and applications of optical remote sensing, pp. 336-428.

LANDSAT-7. (2016). LANDSAT SCIENCE. Retrieved May 5, 2016, from http://landsat.gsfc.nasa.gov/wp-content/uploads/2016/08/Landsat7_Handbook.pdf

OPENSTREETMAP. (2016). OPENSTREETMAP. Retrieved May 5, 2016, from https://www.openstreetmap.org.

Schaffler, A., & Swilling, M. (2013). Valuing green infrastructure in an urban environment under pressure- The Johannesburg case. Ecological economics, pp. 246-247.

Scikit-LBP. (2016). Scikit-LBP. Retrieved June 5, 2016, from http://scikit-image.org/docs/dev/auto_examples/plot_local_binary_pattern.html?highlight=local%20binary%20pattern.

SOUTH-AFRICA. (2016). SOUTHAFRICA INFO. Retrieved May, 2016 from http://www.southafrica.info/news/urbanisation-240113.htm#.V8pUv_l97Z4#ixzz4JAHmoShP.

TERRSAT-LCM. (2016). TERRSAT-LCM. Retrieved June 20, 2016, from https://clarklabs.org/terrset/land-change-modeler/.

USGS. (2016). EARTH-EXPLORER. Retrieved May, 2016, from http://earthexplorer.usgs.gov/.

WIKI-JOHANNESBURG. (2016). WIKI-JOHANNESBURG. Retrieved April 10, 2016, from https://en.wikipedia.org/wiki/Johannesburg.

WORLD-BANK. (2016). WORLD-BANK. Retrieved July 8, 2016, from http://data.worldbank.org/.

Yadav, P., & Deshpande, S. (2015). Spatio-Temporal assessment of urban growth impact in Pune city using remotely sensed data. 36th Asian Conference on Remote Sensing - ACRS.